

## SUPPORTING INFORMATION

### DESIGN OF RUBBER COMPOSITES WITH AUTONOMOUS SELF-HEALING CAPABILITY

Saul Utrera-Barrios; Marianella Hernández Santana\*; Raquel Verdejo; Miguel A. López-Manchado

*Institute of Polymer Science and Technology (ICTP-CSIC), Juan de la Cierva 3, 28006 Madrid, Spain*

\*corresponding author: marherna@ictp.csic.es

#### SI.1. Curing curves and crosslink density of ENR compounds and ENR-TRGO nanocomposites

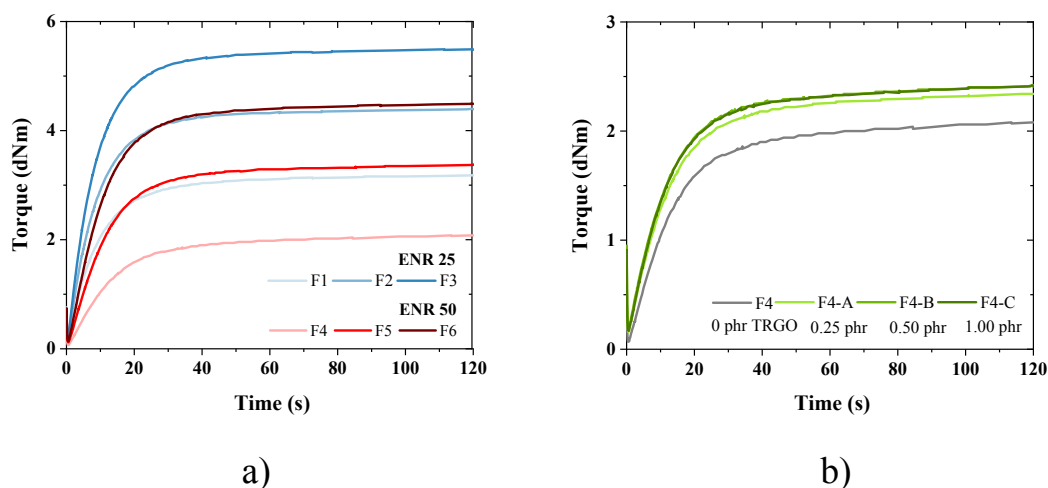


Figure S 1. a) Curing curves of ENR compounds, b) Curing curves of ENR-TRGO nanocomposites.

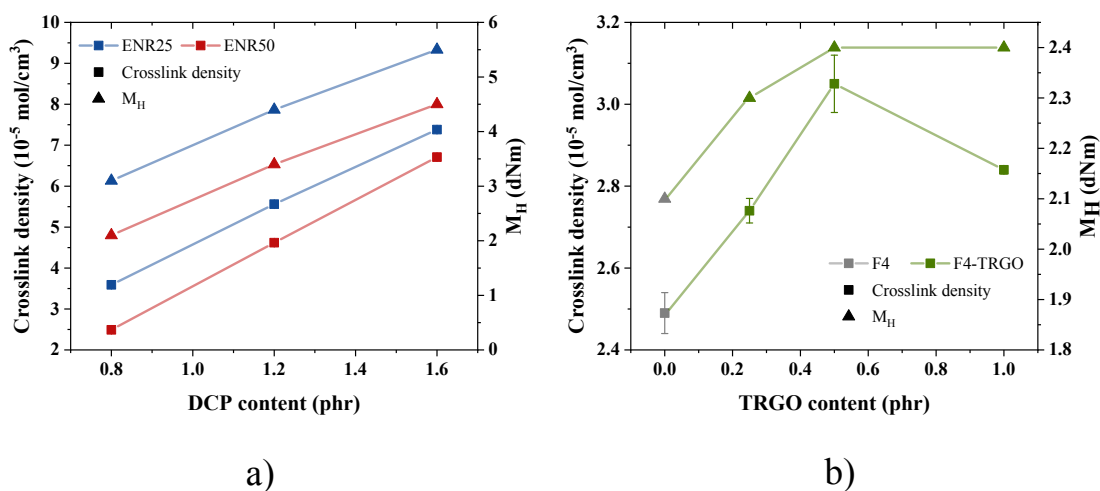


Figure S 2. a) Crosslink density of ENR compounds, b) Crosslink density of ENR-TRGO nanocomposites.

## SI.2. Mechanical properties of ENR compounds.

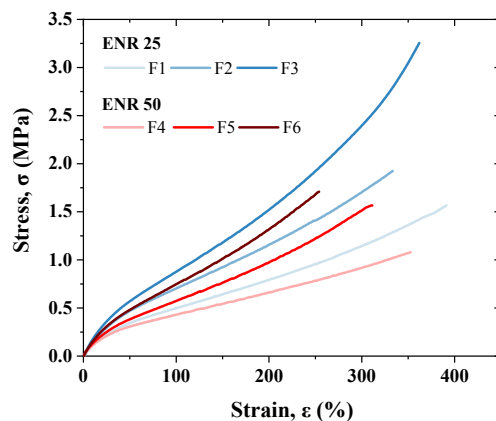


Figure S 3. Stress-strain curves of ENR compounds.

Table S 1. Mechanical properties of ENR compounds.

Compound	$M_H$ (dN.m)	$\nu \cdot 10^{-5}$ (mol/cm <sup>3</sup> )	$M_{100}$ (MPa)	$M_{300}$ (MPa)	$\sigma_R$ (MPa)	$\epsilon_R$ (%)
F1	3.14 ± 0.04	3.59 ± 0.05	0.51 ± 0.01	1.16 ± 0.01	1.58 ± 0.02	394 ± 04
F2	4.36 ± 0.04	5.57 ± 0.03	0.70 ± 0.01	1.70 ± 0.01	1.90 ± 0.04	328 ± 06
F3	5.48 ± 0.01	7.38 ± 0.09	0.87 ± 0.01	2.44 ± 0.05	3.2 ± 0.1	350 ± 12
F4	2.08 ± 0.01	2.49 ± 0.05	0.45 ± 0.02	0.95 ± 0.03	1.08 ± 0.03	349 ± 18
F5	3.38 ± 0.01	4.63 ± 0.02	0.59 ± 0.02	1.52 ± 0.01	1.61 ± 0.05	315 ± 08
F6	4.50 ± 0.00	6.71 ± 0.09	0.76 ± 0.01	2.11 ± 0.01	1.7 ± 0.3	251 ± 35

### SI.3. Infrared spectra of ENR compounds.

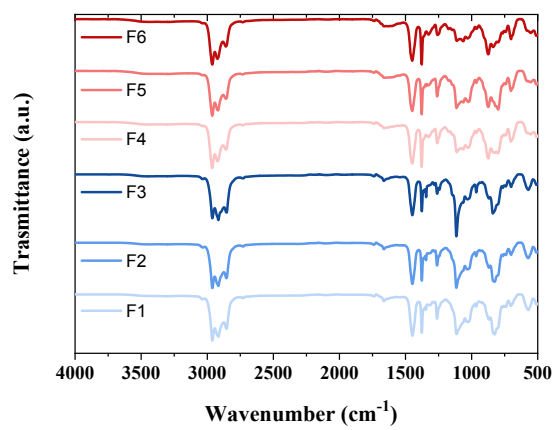


Figure S 4. Infrared spectra of ENR compounds.

#### SI.4. Mechanical properties of ENR-TRGO nanocomposites

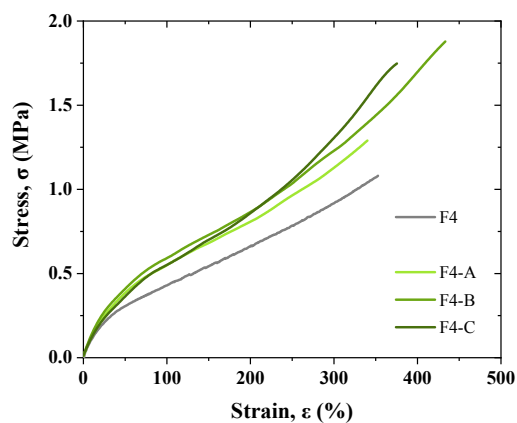


Figure S 5. Stress-strain curves of ENR-TRGO nanocomposites.

Table S 2. Mechanical properties of ENR-TRGO nanocomposites.

<b>Compound</b>	<b><math>M_H</math></b> (dN.m)	<b><math>\nu \cdot 10^{-5}</math></b> (mol/cm <sup>3</sup> )	<b><math>M_{100}</math></b> (MPa)	<b><math>M_{300}</math></b> (MPa)	<b><math>\sigma_R</math></b> (MPa)	<b><math>\epsilon_R</math></b> (%)
F4	2.08 ± 0.01	2.49 ± 0.05	0.45 ± 0.02	0.95 ± 0.03	1.08 ± 0.03	349 ± 18
F4-A	2.32 ± 0.03	2.74 ± 0.03	0.54 ± 0.04	0.94 ± 0.09	1.3 ± 0.2	336 ± 49
F4-B	2.42 ± 0.01	3.05 ± 0.09	0.57 ± 0.01	1.21 ± 0.02	1.85 ± 0.07	431 ± 16
F4-C	2.40 ± 0.02	2.84 ± 0.01	0.56 ± 0.01	1.29 ± 0.02	1.7 ± 0.2	376 ± 33

### SI.5. Stress-strain curves of F4-B before and after healing protocol

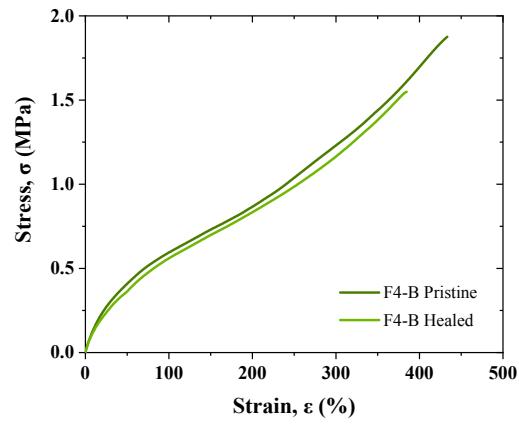


Figure S 6. Stress-strain curves of F4-B before and after healing protocol.

## SI.6. Characterization of TRGO

Raman spectroscopy was carried out in a *Renishaw Invia* Raman Confocal microscope using an argon laser radiation source with an excitation wavelength of 514.5 nm. Three spectra were recorded from 250  $\text{cm}^{-1}$  to 3000  $\text{cm}^{-1}$ . The crystallinity and the disorder in the basal-plane were determined from the area of the peaks of the corresponding bands. FT-IR spectroscopy was used to analyze the TRGO functionalization using potassium bromide (KBr) pellets in a *Perkin Elmer* spectrometer, model UATR Two. Spectra were taken from 400  $\text{cm}^{-1}$  to 4000  $\text{cm}^{-1}$  with a resolution of 4  $\text{cm}^{-1}$ . Pure KBr spectrum was used as background. X-ray photoemission spectroscopy (XPS) analysis was performed on a *Fisons MT500* spectrometer, operated at 300 W, with a non-monochromatized radiation source of  $\text{MgK}\alpha$  of photon energy equal to 1253.36 eV. The deconvolution was done in *Origin Pro*, with a Shirley type baseline and Gaussian adjustment.

Raman spectroscopy is commonly used to analyze the graphitic quality of carbon materials by comparing the intensity ratio between the D, at 1360  $\text{cm}^{-1}$ , and G, at 1580  $\text{cm}^{-1}$ , bands ( $I_D/I_G$ ) (Figure S7). The results reflect the structural changes occurred during the oxidation and exfoliation treatment and show a significant increase in disorder, which is usually attributed to direct damage and functionalization of the surface.

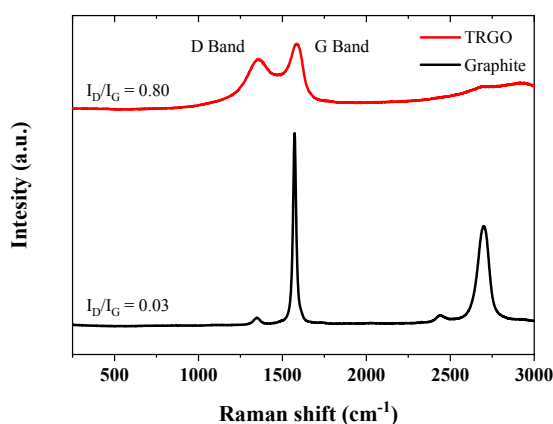


Figure S 7. Raman spectra of graphite and TRGO.

The nature of the functionalization was later established by XPS and FT-IR. The general XPS spectrum (Figure S9) reports the presence of carbon (~75 %) and oxygen (~25 %) atoms, by the relationship between their peaks and the deconvolution of the incorporated functionalities.

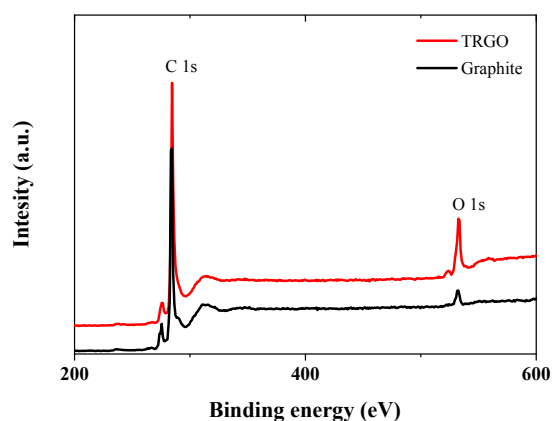


Figure S 8. General XPS spectra of graphite and TRGO.

Figure S3 shows the deconvolution performed on the C 1s and O 1s signals. Figure S9.a presents the deconvolution of the C 1s signal with the percentages of the different species. The components indicate the presence of: non-oxygenated ring C=C ( $sp^2$  hybridization) at 284.5 eV, the C-C ( $sp^3$  hybridization) at 285.8 eV, C-OH bonds at 286.6 eV, C-O-C group at 287.6 eV, carboxylate carbon at 288.8 eV and the  $\pi$ - $\pi^*$  interactions associated to the non-oxygenated ring C=C ( $sp^2$  hybridization) at 291.0 eV, which reveals the success of reduction. The deconvolution performed on the signal of O 1s (Figure S9.b) is consistent with the C 1s data and reveals the presence of C-O bonds (C-OH and C-O-C) at 533.3 eV and the O associated to the carboxylate group at 531.0 eV.<sup>1-2</sup>

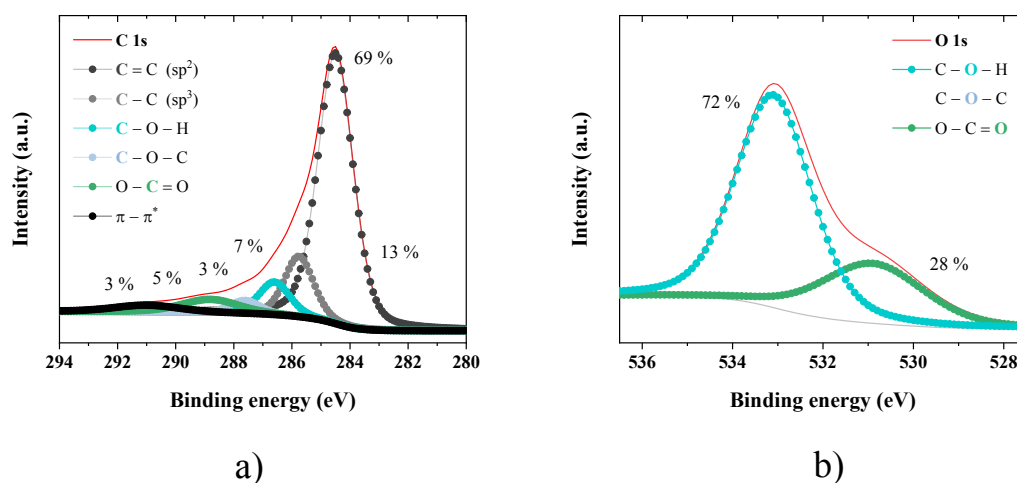


Figure S 9. Peak deconvolution of the a) C 1s and b) O 1s for TRGO.

The functional groups were corroborated by the analysis of their infrared spectrum (Figure S10). Characteristic bands of TRGO were identified at  $3400\text{ cm}^{-1}$  ( $-\text{OH}$  stretching vibration), at  $2960\text{ cm}^{-1}$ ,  $2920\text{ cm}^{-1}$  and  $2860\text{ cm}^{-1}$  ( $-\text{CH}$  stretching vibrations) and at  $1630\text{ cm}^{-1}$  ( $\text{C}=\text{C}$  bending in cyclic bonds). As for the epoxy groups attached to the TRGO cyclic structure, its characteristic peak is identified at  $890\text{ cm}^{-1}$ . A band at  $1110\text{ cm}^{-1}$  is also observed for the symmetrical stretching of type  $\text{C}-\text{O}-\text{C}$ . A small peak is present at  $1740\text{ cm}^{-1}$  associated with carboxylic groups, coinciding with XPS data.<sup>3</sup>

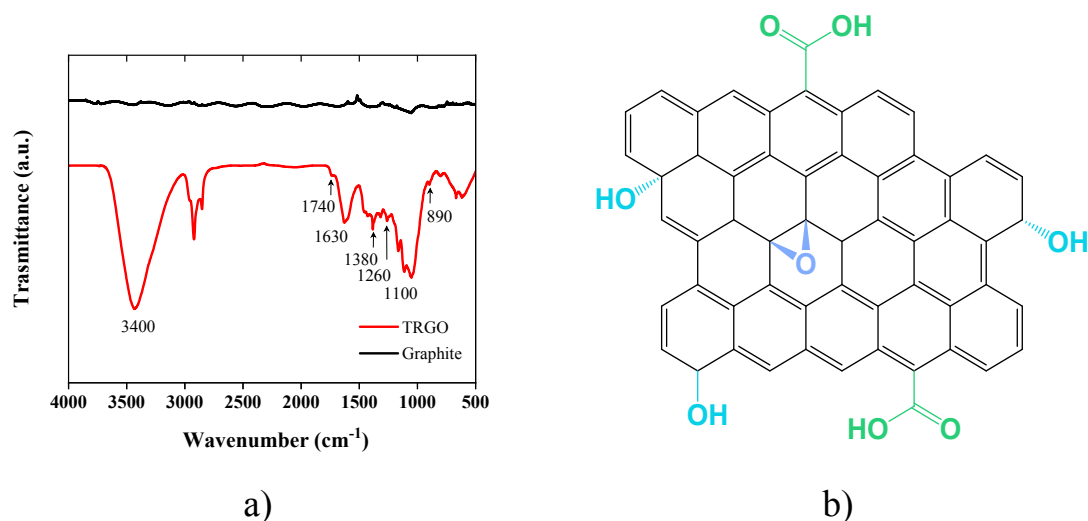


Figure S 10. a) FT-IR spectrum of graphite; b) scheme of TRGO with its functional group.

## REFERENCES

1. Stankovich, S.; Piner, R. D.; Chen, X.; Wu, N.; Nguyen, S. T.; Ruoff, R. S., Stable aqueous dispersions of graphitic nanoplatelets via the reduction of exfoliated graphite oxide in the presence of poly (sodium 4-styrenesulfonate). *J. Mater. Chem.* **2006**, *16* (2), 155-158.
2. Botas, C.; Álvarez, P.; Blanco, P.; Granda, M.; Blanco, C.; Santamaría, R.; Romasanta, L. J.; Verdejo, R.; López-Manchado, M. A.; Menéndez, R., Graphene materials with different structures prepared from the same graphite by the Hummers and Brodie methods. *Carbon* **2013**, *65*, 156-164.
3. Socrates, G., *Infrared and Raman Characteristic Group Frequencies*. 3rd ed.; John Wiley & Sons, LTD: England, 2001; pp 1-347.